EC
Journals.ASM.org

The Volatome of *Aspergillus fumigatus*

C. Heddergott,[a] A. M. Calvo,[b] J. P. Latgé[a]

Unité des Aspergillus, Institut Pasteur, Paris, France[a]; Department of Biological Sciences, Northern Illinois University, Dekalb, Illinois, USA[b]

Early detection of invasive aspergillosis is absolutely required for efficient therapy of this fungal infection. The identification of fungal volatiles in patient breath can be an alternative for the detection of *Aspergillus fumigatus* that still remains problematic. In this work, we investigated the production of volatile organic compounds (VOCs) by *A. fumigatus in vitro*, and we show that volatile production depends on the nutritional environment. *A. fumigatus* produces a multiplicity of VOCs, predominantly terpenes and related compounds. The production of sesquiterpenoid compounds was found to be strongly induced by increased iron concentrations and certain drugs, i.e., pravastatin. Terpenes that were always detectable in large amounts were α-pinene, camphene, and limonene, as well as sesquiterpenes, identified as α-bergamotene and β-*trans*-bergamotene. Other substance classes that were found to be present in the volatome, such as 1-octen-3-ol, 3-octanone, and pyrazines, were found only under specific growth conditions. Drugs that interfere with the terpene biosynthesis pathway influenced the composition of the fungal volatome, and most notably, a block of sesquiterpene biosynthesis by the bisphosphonate alendronate fundamentally changed the VOC composition. Using deletion mutants, we also show that a terpene cyclase and a putative kaurene synthase are essential for the synthesis of volatile terpenes by *A. fumigatus*. The present analysis of *in vitro* volatile production by *A. fumigatus* suggests that VOCs may be used in the diagnosis of infections caused by this fungus.

Aspergillus fumigatus is an opportunistic fungal pathogen that causes life-threatening invasive pulmonary infections (invasive aspergillosis [IA]) among immunocompromised patients. A sensitive, rapid, and accurate diagnostic assay for invasive aspergillosis is required to successfully fight this fungal infection (1). It has recently been proposed that the detection of volatiles can be used for the diagnosis of pulmonary infections (2, 3) and lung cancer (4, 5). Several aspergilli, including *A. flavus*, *A. ustus*, and *A. versicolor*, have been identified within the scope of environmental studies, where room air was analyzed to detect fungal pollution in houses (6–8). 2-Pentylfuran (2-PF) was detected in the breath of patients with *A. fumigatus* infection (9). It was shown that *A. fumigatus* produces farnesene when grown *in vitro* (10), and the use of terpene volatiles for the detection of IA has recently been proposed (11). However, the spectrum of volatile organic compounds (VOCs) produced by *A. fumigatus* and their synthesis have been poorly described. In this work, we characterized the patterns of volatile terpenes produced *in vitro* by *A. fumigatus* during growth under saprophytic conditions. In addition, the molecular pathways responsible for the synthesis of terpenoid volatiles were defined.

MATERIALS AND METHODS

Strains. *Aspergillus fumigatus* strain FGSC A1163 (= DAL = CBS144.89) was used for wild type strain-based experiments. Gene deletions were obtained on a CEA17 *akuB*^{KU80} background (12). A terpene cyclase mutant (the *AFUA_8G00520* = *AFUB_086050* mutant) has been already described (13). To generate a mutant with a deletion of the gene encoding the putative terpene synthase family protein AFUB_062550 (AFUA_5G15060), up- and downstream flanking regions obtained with the primers 62550up-fwd (5′-ATTCGAGCTCGGTACGATATCTTATCACATCGCCTGTCAACC-3′), 62550up-rev (5′-GGACCTGAGTGATGCATGTCTGGCGTAGGCTTTGC-3′), 62550do-fwd (5′-TGGTCCATCTAGTGCCCACAGCGATGTGATATGCAG-3′), and 62550do-rev (5′-CCAAGCTTGCATGCCGATATCATCCACAAGCAAGCAGCACAG-3′) were cloned into the pUC19 vector together with the beta-rec/*six* Hph^r recyclable hygromycin resistance cassette (14) using a GeneArt seamless cloning and assembly kit (Life Technologies). The construct was transformed into *A. fumigatus* CEA17 *akuB*^{KU80} as described elsewhere (15).

Culture conditions. Fungal conidia were harvested from 7-day-old malt agar slants (2% [wt/vol] malt extract [Difal, France], 2% [wt/vol] agar-agar [Sobigel, France]) using a 0.05% (vol/vol) Tween 20 (Prolabo, France) solution in water. Headspace vials with septate caps (40 ml; Sigma-Aldrich) were cleaned by rinsing vigorously with ethanol and then rinsing two times with deionized water before use. After autoclaving, the vials were filled with 5 ml of medium. Conidia were added at a final concentration of 10^6/ml. The sealed vials were then incubated without shaking at 37°C in an incubator, and the standard cultivation time was 48 h. For dry weight determination, mycelia were harvested onto round filters (no. 4; diameter, 55 mm; Macherey-Nagel) using vacuum filtration, extensively washed with water, and dried at 50°C. We verified that the use of sealed vials did not limit growth in our septate vials with Brian's medium, since fungal biomass increased up to day 3 of cultivation. Therefore, our sampling time of 48 h occurred during the active phase of growth. To analyze samples grown under aerated conditions, the polytetrafluoroethylene septum was replaced by permeable stoppers (Hirschmann, Germany). Growth in a fermentor was performed using 1 liter *Aspergillus* minimal medium (AMM; see below). One hundred milliliters of 24-h-old AMM preculture inoculated with 10^6 conidia per ml was used as a starter culture; the fermentation was performed under stirring (300 rpm) and aeration at a rate of 0.5 liter/min.

Media and additives. Three defined media were preassayed in terms of their suitability to VOC analysis: Brian's broth (16), AMM (17), and RPMI 1640 (Sigma-Aldrich) supplemented with 0.3 g/liter glutamine and buffered to pH 7.0 with 0.165 M morpholinepropanesulfonic acid

Received 24 March 2014 Accepted 27 May 2014
Published ahead of print 6 June 2014
Address correspondence to C. Heddergott, christoph.heddergott@pasteur.fr.
Supplemental material for this article may be found at http://dx.doi.org/10.1128/EC.00074-14.

doi:10.1128/EC.00074-14

(MOPS; Sigma-Aldrich) (18). Brian's medium contains (per liter) 50 g D-glucose, 10 g L-asparagine, 2.4 g NH_4NO_3, 10 g KH_2PO_4, 2 g $MgSO_4 \cdot 7H_2O$, 1.3 ml of a 5% (wt/vol) $CaCl_2$ solution, and 1.3 ml of a trace element solution containing 2% (wt/vol) $ZnSO_4 \cdot 7H_2O$, 0.2% (wt/vol) $CuSO_4 \cdot 5H_2O$, 0.1% (wt/vol) $Co(NO_3)_2 \cdot 6H_2O$, and 0.08% (wt/vol) $FePO_4$. The pH was set to 5.4. AMM was prepared using 6 g/liter sodium nitrate as the sole nitrogen source. All media were filter sterilized using a 0.2-μm-pore-size syringe filter (Sartorius, Germany) or a Stericup/Steritop system (Millipore). Brian's broth components were prepared as a 2× stock (pH 5.4). Final reconstitution of Brian's medium was performed by combining the 2× concentrate, water, and (if applicable) the drug/compound stock solutions. Metals were added as salt solutions in water. $CuCl_2$, $Fe_2(SO_4)_3$, $FeSO_4$, and $MnCl_2$ were added at a final concentration of 100 μM, and 1 mM $ZnSO_4 \cdot 7\ H_2O$ was used. Preliminary assays have shown the same volatile patterns in AMM, RPMI 1640, and Brian's broth. Brian's medium was selected for use for determination of the volatome composition in solid-phase microextraction (SPME) vial experiments because it induced the highest levels of mycelial growth. Drug stocks were prepared as follows: pravastatin (Sigma-Aldrich), 1 mg/ml in water; alendronate (Sigma-Aldrich), 10 mg/ml in water; voriconazole (Sigma-Aldrich), 1 mg/ml stock in ethanol; and menadione (Sigma-Aldrich), 10 mg/ml in ethanol. They were used in a range of final concentrations that affect growth (16.6 to 125 μg/ml pravastatin, 78 to 1,250 μg/ml alendronate, 78 to 1,250 ng/ml voriconazole, and 0.5 to 4 μg/ml menadione).

SPME and GC. Fungal volatile extraction and analysis were carried out as described elsewhere (7), with modifications. The SPME fiber assembly divinylbenzene (DVB)-carboxene (CAR)-polydimethylsiloxane (PDMS) (Sigma-Aldrich) was used for volatile extraction. Beside the carboxene-DVB-PDMS copolymer fiber, other coatings (7 μm PDMS, 100 μm PDMS, 85 μm polyacrylate from SPME fiber assortment kit 1; Sigma-Aldrich) were assayed, but they have been less efficient than the copolymer because the surface has less of a coating and limited affinities due to the coating by a single polymer instead of the three polymers in the DVB-CAR-PDMS fiber. As control analytes, stocks of 1% (vol/vol) terpene standards (α-pinene [Sigma-Aldrich], camphene [Sigma-Aldrich], D-limonene [Sigma-Aldrich], β-*trans*-bergamotene (13), and a mixture of farnesene isomers [Sigma-Aldrich]) were prepared at 1% (vol/vol) in tetrahydrofuran (THF; Sigma-Aldrich). From these stocks, 100 ppm α-pinene, camphene, D-limonene, and β-*trans*-bergamotene and 1,000 ppm farnesene isomer mix were prepared in methanol.

The SPME fiber was mounted in a fiber holder for manual sampling (Sigma-Aldrich). After piercing the septum, the needle was protruded 2.5 cm into the headspace of the culture vial (40 ml; Sigma-Aldrich). The 2-cm coated fiber was exposed at full length for 30 min at 37°C and immediately submitted to measurement by gas chromatography (GC). In SPME mock-ups obtained with the terpene control analytes, we found that about 90% of these standards were extracted within 30 min; this amount was equal to that achieved with longer extraction periods. Thus, for maximal sample throughput, a 30-min extraction time was used for all experiments. For fiber desorption, the inlet port of the Agilent 7890A GC system was used together with a SPME inlet liner (78.5 by 6.5 by 0.75 mm; Sigma-Aldrich). The fiber was desorbed at 250°C with an injection pulse pressure of 25 lb/in^2 for 2 min. Between two extractions, the fiber was left in the injection port for 15 min to ensure complete desorption and to perform fiber conditioning. Using this desorption time, no carryover of volatiles was observed. After each day (12 to 15 SPMEs), the fiber was additionally cleaned by heating it to 270°C for 30 min. Each fiber was used for approximately 100 extractions, and no reduction in quality was observed during that time. GC/mass spectrometry (MS) analysis was carried out on an Agilent 7890A GC system coupled to an Agilent 5975C inert XL EI/CI MSD mass spectrometer. After injection/fiber desorption, volatiles were separated on an Agilent J&W HP-5ms GC column (30 m by 0.25 mm by 0.25 μm) under helium flow (1.1971 ml/min). The oven heat ramp was 30°C for 4 min and then 10°C/min to 100°C, 3°C/min to 150°C, and 15°C/min to 250°C for 3 min. For the analysis of diterpenes, an alternative program was used (40°C initial temperature, 9°C/min to 229°C, and 36°C/min to 265°C with a hold for 5 min; 27 min in total). MS signals (electron impact [EI] mode) were acquired in a mass range of 40 to 500 Da. Data analysis was carried out using MSD ChemStation software (v.E02.01.1177; Agilent). Signals were integrated with an RTE integrator. Peaks were identified using the NIST database (v.8), and the compound names given in Table 1 refer to these identifications. For statistical analysis, peak area values from 3 triplicate experiments were compared using Student's 2-sided *t* test.

RESULTS

Volatome composition. The reference VOC profile was obtained upon cultivation in Brian's medium using septate vials, as described in the Materials and Methods section. The volatome was almost exclusively composed of monoterpenes and sesquiterpenes. The GC profile of the *A. fumigatus* volatome on Brian's medium is shown in Fig. 1A to C, peak identifications are listed in Table 1, and the corresponding EI spectra are listed in Table S1 in the supplemental material. Figure 1A shows the whole GC profile for growth on Brian's medium and medium supplemented with 100 μM iron. Figures 1B and C show rescaled sections to visualize the VOCs present in a lower abundance. Background signals that originated from the GC column, the SPME fiber, or the lab ware that was used, mostly dimethylsiloxanes, were determined by control measurements and are labeled with the ¤ symbol. Figure S1 in the supplemental material shows a control measurement obtained using Brian's medium without inoculation; identifications for the contaminants therein are given in Table S2 in the supplemental material. In our GC programs, their signals did not interfere with those of compounds produced by the fungus. VOC signals were identified by submitting the EI fragment mass spectra obtained to an NIST database search. The spectrum of each peak together with the spectrum of the most probable compound from the database is shown in Table S1 in the supplemental material. Several substance searches did not lead to significant hits.

The monoterpenes unambiguously identified were α-pinene (peak 4), camphene (peak 5), and D-limonene (peak 8), since commercial standards were used to verify retention times and EI fragmentation patterns. These data also show that low probability scores were not prejudicial to a correct identification, since standard pinene and limonene were identified with low scores of about 10 to 15%. Compound 9 was absent from the NIST database, and other putative monoterpenes (peaks 6, 7, and 10a) were present in small amounts.

The major VOC (peak 16) was identified as β-farnesene or *Z*-β-farnesene with a low probability score. Recently, it was shown that β-*trans*-bergamotene is the major sesquiterpene of *A. fumigatus* (13). This terpene is not present in the NIST (v.8) database, but the ion spectra and retention times of the VOC at peak 16 and the β-*trans*-bergamotene standard were identical. The second-most-abundant VOC (peak 13) was identified as its isomer, α-bergamotene. Other putative sesquiterpene signals present in Brian's medium cultures were 8,9-dehydro-cycloisolongifolene (peak 11), α-santalene (peak 12), (−)-β-santalene (peak 14), β-bisabolene (peak 17), 4,5,9,10-dehydro-isolongifolene (peak 18a), and β-vatirenene (peak 18b). The VOC at peak 15 was not found in the NIST database.

Conditions affecting VOC production. (i) Cation supplementation. The addition of iron to the culture medium highly stimulated the production of terpenes (Fig. 1A to C, BRI/FE chromatograms). The maximal stimulation was observed with 100 μM

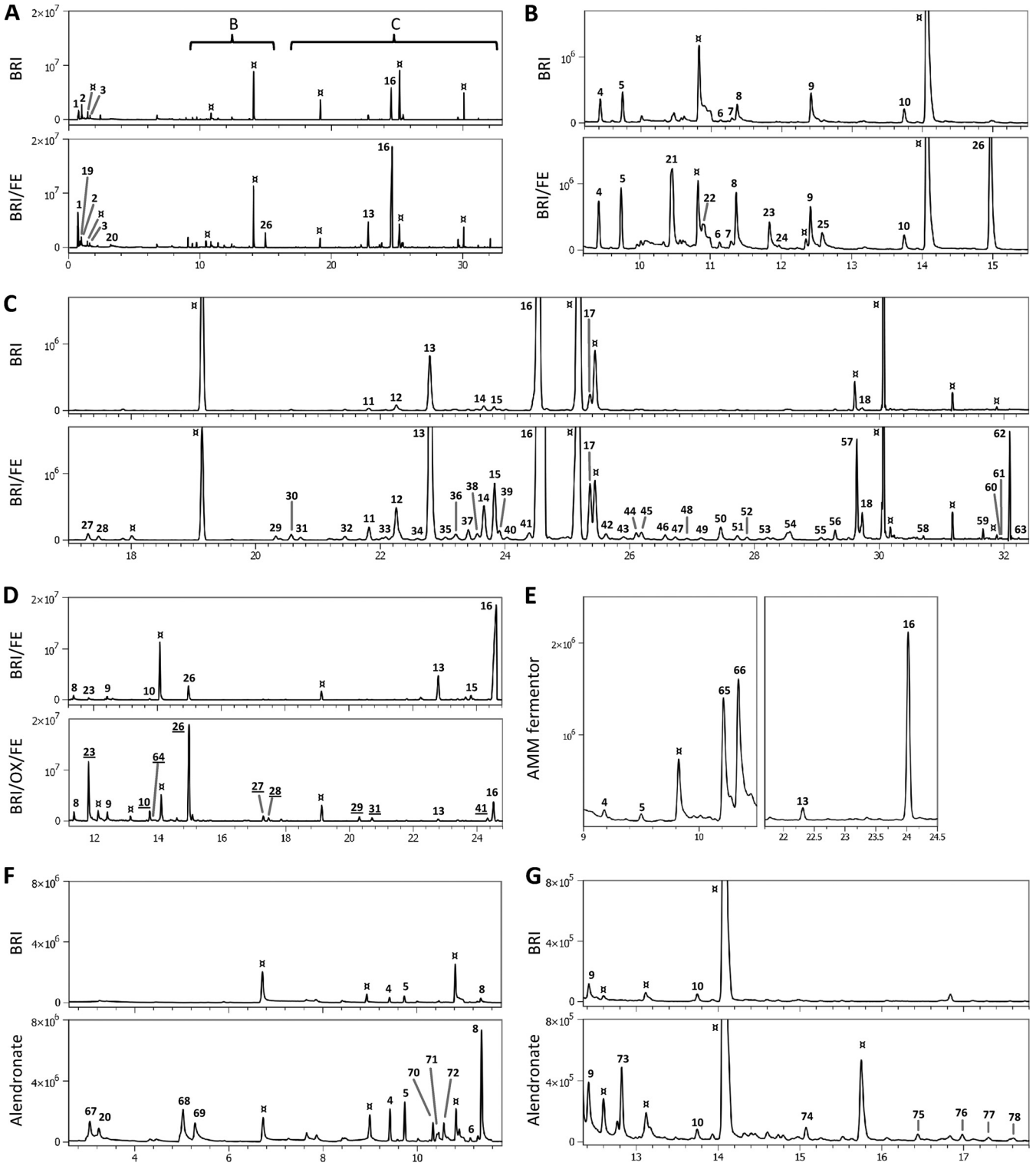

FIG 1 VOCs produced by *Aspergillus fumigatus*. *x* axes, time (in minutes); *y* axes, ion count. Contaminants, mostly dimethylsiloxanes, are indicated by the ¤ symbol. (A to C) VOCs produced on Brian's broth (BRI). (A) The whole chromatogram and early volatiles. The brackets marked B and C indicate those sections for which detailed views of the profile are given in panels B (9.2 to 15.5 min) and C (17 to 32.4 min), respectively. Upper GC profiles, Brian's broth with a normal iron concentration (4.6 μM) (BRI); lower profiles, Brian's broth with an iron concentration of 100 μM (BRI/FE). (D) Specific upregulation of VOCs (underlined) in the presence of iron and oxygen (BRI/FE/OX) compared to the regulation in the septate vial setup (BRI/FE). (E) Volatiles produced during growth in a fermentor containing minimal medium and detected in the headspace of the fermentation vessel. (F, G) Specific production of terpenoid metabolites in the presence of alendronate compared to that in Brian's broth without the drug. The two sections of the chromatogram have different scales to visualize the peaks with a low abundance (peaks 74 to 78).

TABLE 1 VOCs detected in the volatome of *A. fumigatus*[a]

VOC type and peak no.	R_T (min)	Formula	Trivial name	CAS no.	NIST database accession no.	Substance class	Probability	Panel(s) in Fig. 1
VOCs produced upon growth on Brian's medium								
1	0.764	CO_2	Carbon dioxide	124-38-9	ML 13702		2.04	A
2	0.99	C_5H_8	Isoprene	78-79-5	ML 118709	Diene	3.74	A
3	1.615	C_6H_{10}	(*Z*,*Z*)-2,4-Hexadiene	6108-61-8	RL 158233	Diene	15.3	A
4	9.421	$C_{10}H_{16}$	α-Pinene	80-56-8	ML 157903	Monoterpene	15.7	B, E, F
5	9.739	$C_{10}H_{16}$	Camphene	79-92-5	RL 235820	Monoterpene	45.9	B, E, F
6	11.134	$C_{10}H_{16}$	Terpinolene	586-62-9	ML 114838	Monoterpene	28.1	B, F
7	11.298	$C_{10}H_{16}$	*o*-Cymene	527-84-4	RL 57776	Monoterpene	28.8	B
8	11.369	$C_{10}H_{16}$	D-(+)-Limonene	5989-27-5	ML 229344	Monoterpene	9.46	B, D, F
9	12.419							B, D, G
10a	13.738	$C_{10}H_{16}$	γ-Terpinen	99-85-4	RL 34195	Monoterpene	13.1	B, D, G
10b	13.738	$C_9H_{14}N_2$	2,3-Diethyl-5-methyl-pyrazine	18138-04-0	ML 236562	Pyrazine	24	B, D, G
11	21.821	$C_{15}H_{22}$	8,9-Dehydro-cycloisolongifolene		ML 151280	Sesquiterpene	24.9	C
12	22.251	$C_{15}H_{24}$	α-Santalene	512-61-8	RL 141043	Sesquiterpene	58.5	C
13	22.805	$C_{15}H_{24}$	α-Bergamotene	17699-05-7	ML 141044	Sesquiterpene	54.9	A, C, D, E
14	23.657	$C_{15}H_{24}$	(−)-β-Santalene	511-59-1	RL 9213	Sesquiterpene	67.2	C
15	23.8							C, D
16	24.539	$C_{15}H_{24}$	β-*trans*-Bergamotene	28973-97-9	ML 141110	Sesquiterpene	10.9	A, C, D, E
17	25.395	$C_{15}H_{24}$	β-Bisabolene	495-61-4	ML 9219	Sesquiterpene	41.2	C
18a	29.708	$C_{15}H_{23}$	4,5,9,10-Dehydro-isolongifolene	156747-45-4	ML 151550	Sesquiterpene	71.7	C
18b	29.728	$C_{15}H_{24}$	β-Vatirenene		ML 293042	Sesquiterpene	34.6	C
Additional VOCs produced in iron-supplemented cultures								
19	0.887	C_2H_6O	Ethanol	64-17-5	ML 118507	Alcohol	90.5	A
20	3.236	$C_5H_{12}O$	3-Methyl-1-butanol	123-51-3	RL 227760	Alcohol	76.9	A, F
21	10.457	C_9H_{14}	3-Ethylidenecycloheptene		ML 211167		17.9	B
22	10.888	$C_{10}H_{16}$	α-Phellandrene	99-83-2	RL 3305	Monoterpene	61.5	B
23	11.841	$C_8H_{12}N_2$	2-Methyl-5-isopropylpyrazine	13925-05-8	ML 3375	Pyrazine	64.4	B, D
24	11.975	$C_{10}H_{16}$	α-Phellandrene	99-83-2	RL 118210	Monoterpene	33	B
25a	12.58	$C_9H_{18}O$	(*E*)-6-Nonen-1-ol	31502-19-9	ML 3861		28.5	B
25b	12.6	$C_{10}H_{16}$	Terpinolen	586-62-9	ML 114838	Monoterpene	23.6	B
26	14.97							A, B, D
27	17.298							C, D
28	17.462	$C_{11}H_{18}N_2$	2-(2-Methylpropyl)-3-(1-methylethyl)pyrazine		ML 108603	Pyrazine	81.2	C, D
29	20.323							C, D
30	20.518	$C_{15}H_{24}$	(*Z*,*E*)-α-Farnesene	26560-14-5	RL 22554	Sesquiterpene	20.2	C
31	20.754							C, D
32	21.431							C
33	22.087	$C_{15}H_{24}$	Cedr-8(15)-ene	11028-42-5	ML 141090	Sesquiterpene	11.6	C
34	22.6	$C_{15}H_{24}$	α-Curcumene	644-30-4	ML 249520	Sesquiterpene	53.2	C
35	23.031							C
36a	23.144	$C_{15}H_{24}$	Dihydrocurcumene	1461-02-5	ML 151304	Sesquiterpene	46.6	C
36b	23.226	$C_{15}H_{24}$	(+)-Epi-β-santalene	25532-78-9	RL 9212	Sesquiterpene	43.6	C
37	23.41							C

38	23.554	$C_{15}H_{24}$	NA	79718-83-5	ML 195379	Sesquiterpene	39.2	C
39	23.944							C
40	24.016	$C_{15}H_{24}$	α-Curcumene	644-30-4	RL 141047	Sesquiterpene	42.1	C
41	24.334	$C_{10}H_{10}O_5$	2,4-Diacetylphloroglucinol	2161-86-6	ML 9727	Polyketide	70.9	C, D
42	25.616							C
43	25.903							C
44	26.108							C
45	26.19	$C_{15}H_{24}$	α-Patchoulene	560-32-7	ML 22532	Sesquiterpene	20.9	C
46	26.569	$C_{15}H_{24}$	*cis*-α-Bisabolene	29837-07-8	ML 293017	Sesquiterpene	26.1	C
47	26.733							C
48	26.908							C
49	27.144	$C_{15}H_{24}$	β-Vatirenene		ML 293042	Sesquiterpene	19.1	C
50	27.462							C
51	27.728	$C_{15}H_{20}$	4,5,9,10-Dehydro-isolongifolene	156747-45-4	ML 151550	Sesquiterpene	74.8	C
52	27.882							C
53	28.21							C
54	28.6	$C_{15}H_{24}O$	Ledene oxide(II)		ML 159367	Sesquiterpene	20.3	C
55	29.072							C
56	29.298	$C_{15}H_{20}$	4,5,9,10-Dehydro-isolongifolene	156747-45-4	ML 151550	Sesquiterpene	79.9	C
57	29.646	$C_{15}H_{24}O$	Isoaromadendrene epoxide		ML 159366	Sesquiterpene	12.1	C
58	30.713	$C_{15}H_{24}O$	Santalol	11031-45-1	ML 22687	Sesquiterpene	17.6	C
59	31.667	$C_{20}H_{32}$	Biformene	5957-33-5	ML 13164	Diterpene	37.1	C
60	31.933	$C_{20}H_{31}$	Rimuene	1686-67-5	ML 13163	Diterpene	22.1	C
61	31.964	$C_{20}H_{32}$	(5α,9α,10β)-Kaur-15-ene	511-85-3	RL 13170	Diterpene	77.2	C
62	32.098	$C_{20}H_{32}$	13-Isopimaradiene	1686-56-2	ML 42568	Diterpene	55.3	C
63	32.241	$C_{20}H_{32}$	(8β,13β)-Kaur-16-ene	20070-61-5	RL 13171	Diterpene	42.8	C
Additional VOCs produced in aerated cultures								
64	13.841	$C_9H_{14}N_2$	2-Isobutyl-3-methylpyrazine	13925-06-9	RL 108595	Pyrazine	75	D
65	10.416	$C_8H_{16}O$	1-Octen-3-ol	3391-86-4	ML 352751	Alcohol	89.3	E
66	10.559	$C_8H_{16}O$	3-Octanone	106-68-3	RL 163610	Ketone	71.3	E
Additional VOCs produced in the presence of alendronate								
67	3.052	$C_5H_{10}O$	3-Methyl-3-buten-1-ol, isoprenol	763-32-6	RL 114440	Alcohol	81	F
68	5.031	$C_5H_{10}O$	3-Methyl-2-buten-1-ol, prenol	556-82-1	ML 352701	Alcohol	78	F
69	5.277	C_5H_8O	3-Methyl-2-butenal	107-86-8	ML 190005	Aldehyde	64.6	F
70	10.334	$C_{10}H_{16}$	(−)-β-Pinene	18172-67-3	RL 113186	Monoterpene	36.8	F
71	10.457	$C_5H_{10}O_3$	3-Hydroxy-3-methyl-butanoic acid	625-08-1	RL 279739	Carboxylic acid	86	F
72	10.57	$C_8H_{14}O$	6-Methyl-5-hepten-2-one	110-93-0	RL 230027	Ketone	74.5	F
73	12.826	$C_{10}H_{18}O$	β-Linalool	78-70-6	ML 352637	Monoterpenoid	60.7	H
74	15.072	$C_{10}H_{18}O$	(−)-α-Terpineol	10482-56-1	RL 36610	Monoterpene	39.8	H
75	16.436	$C_{10}H_{16}O$	3,7-Dimethyl-(*Z*)-2,6-octadienal, citral	106-26-3	RL 4798	Monoterpene	44.6	H
76	16.98	$C_{11}H_{20}O_2$	(S)-(−)-Citronellic acid, methyl ester		ML 333551	Monoterpene	98.5	H
77	17.308	$C_{10}H_{16}O$	3,7-Dimethyl-(*Z*)-2,6-octadienal, citral	106-26-3	RL 290609	Monoterpene	37.4	H
78	17.606	$C_{11}H_{18}O_2$	*cis*-Geranic acid methyl ester	1862-61-9	ML 47147	Monoterpene	84	H

[a] NIST database references are given for the mainlib (ML) or replib (RL) database. The given identifications, trivial names, and probabilities of identification are in accord with the NIST database search result. The last column indicates the panels in Fig. 1 showing chromatograms that contain the compound peak. R_T, retention time; NA, not available.

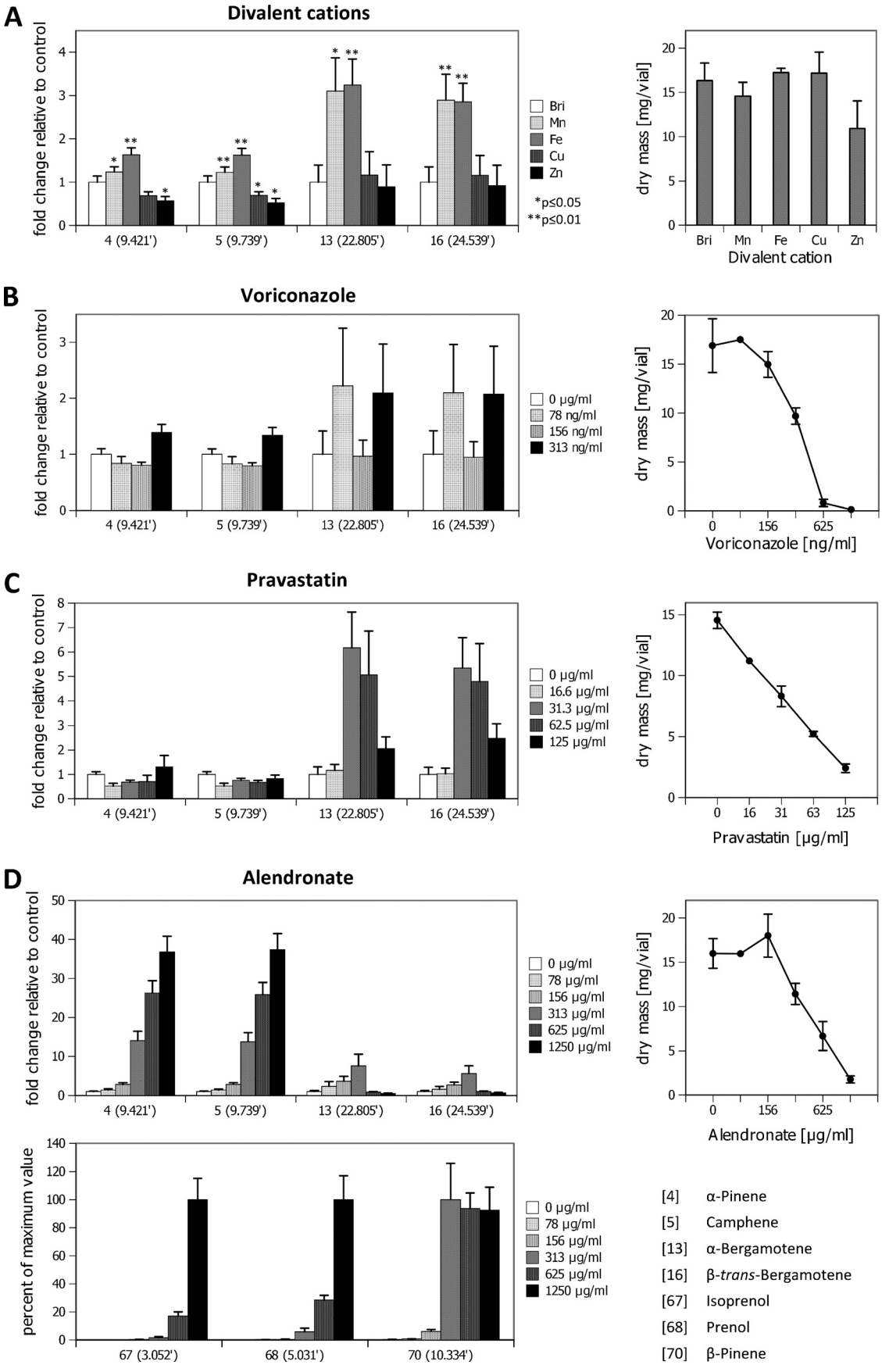
A
Divalent cations
fold change relative to control
4 (9.421')
5 (9.739')
13 (22.805')
16 (24.539')
Bri
Mn
Fe
Cu
Zn
*p≤0.05
**p≤0.01
dry mass [mg/vial]
Bri
Mn
Fe
Cu
Zn
Divalent cation
B
Voriconazole
fold change relative to control
0 µg/ml
78 ng/ml
156 ng/ml
313 ng/ml
dry mass [mg/vial]
0
156
625
Voriconazole [ng/ml]
C
Pravastatin
fold change relative to control
0 µg/ml
16.6 µg/ml
31.3 µg/ml
62.5 µg/ml
125 µg/ml
dry mass [mg/vial]
0
16
31
63
125
Pravastatin [µg/ml]
D
Alendronate
fold change relative to control
0 µg/ml
78 µg/ml
156 µg/ml
313 µg/ml
625 µg/ml
1250 µg/ml
dry mass [mg/vial]
0
156
625
Alendronate [µg/ml]
percent of maximum value
67 (3.052')
68 (5.031')
70 (10.334')
[4] α-Pinene
[5] Camphene
[13] α-Bergamotene
[16] β-*trans*-Bergamotene
[67] Isoprenol
[68] Prenol
[70] β-Pinene

iron (data not shown). A further increase to 1 mM had no effect, and there was no difference observed between Fe^{2+} and Fe^{3+} (data not shown). The addition of iron did not fundamentally change the terpene composition of the volatome or the produced biomass, but overall it stimulated the release of terpenes in larger amounts, especially sesquiterpenes. The relative proportion between the signals of terpenes with equal chain lengths remained constant. For example, the absolute peak volume of camphene (peak 5) throughout the study was approximately 25% higher than that of α-pinene (peak 4), and the peak volume ratio between sesquiterpenes 16 and 13 was about 8 with or without iron supplementation. The larger amount of terpenes produced in iron-enriched samples allowed us to identify compounds that were present in trace amounts in the nonsupplemented medium. After iron supplementation, 47 additional signals were detected, and a multiplicity of them identified as terpenes (3 monoterpenes, 15 sesquiterpenes, and 5 diterpenes [Table 1]).

VOCs that are not terpenes were also found in iron-enriched cultures. The compounds at peaks 23 and 28 were identified as pyrazines, and in iron-enriched cultures, peak 10 contained a putative pyrazine signal (peak 10b) that coeluted with the monoterpene compound (peak 10a) present in medium without iron supplementation. Peak 41 was identified as 2,4-diacetylphloroglucinol, a product of polyketide biosynthesis.

Addition of manganese caused effects similar to the ones seen with iron supplementation, but to a lesser extent. The induction of sesquiterpene release was similar to that achieved with iron supplementation, but the monoterpenes induced by iron were less induced by manganese (Fig. 2A). In contrast to iron and manganese, Cu^{2+} (100 μM and 1 mM) and Zn^{2+} (1 mM) did not stimulate the volatome composition; on the contrary, they slightly reduced monoterpene release (Fig. 2A).

(ii) Aeration. Under aerated growth conditions, the amount of terpene VOCs collected after 30 min was low (Fig. 1D, peaks 13, 15, and 16). However, when an SPME fiber was exposed during 48 h of culture, the same amounts of terpenes were collected from plugged and septate vials. That indicates that the production of terpenes itself was not affected by the presence of oxygen but they were partially lost by evaporation through the permeable plug (data not shown). In contrast, the abundance of volatiles that were not identified as terpenes and that were specific for iron-enriched cultures was substantially increased when *A. fumigatus* grew in aerated cultures (Fig. 1D, peaks 23, 10, 64, 26 to 29, 31, and 41).

Under shake and aerated growth conditions (in a fermentor with AMM and aeration of 0.5 volume of air/volume of medium/min), the signals of abundant terpenes (peaks 4, 5, 13, and 16) were present in samples extracted from the culture vessel headspace. In addition, 1-octen-3-ol (peak 65) and 3-octanone (peak 66) were detected (Fig. 1E). Their concentrations increased over time (see Fig. S2A in the supplemental material), and the compounds were also present in the condensate collected in a chilled trap (4°C) that was analyzed using SPME-GC/MS (see Fig. S2B in the supplemental material). In contrast, no terpenes were extracted from the fermentor condensates (shown in Fig. S2C in the supplemental material for β-*trans*-bergamotene).

Inhibition of terpene VOC biosynthesis. (i) Drugs. Inhibition of the mevalonate pathway that is upstream of the terpene biosynthesis pathway was investigated by addition of statins to the culture medium. Addition of pravastatin (Fig. 2C) and simvastatin (data not shown) at moderately inhibitory concentrations unexpectedly resulted in a substantial increase in sesquiterpene production, whereas monoterpene levels remained unchanged. Even at concentrations causing high levels of growth inhibition (≥62.5 μg/ml), terpene signals were detectable, and the weight-corrected sesquiterpene production level did not drop below the control values. No volatome alterations (e.g., novel compounds) were observed, and the sesquiterpene induction pattern was very similar to the one seen with Fe and Mn supplementation.

The bisphosphonate alendronate blocks the synthesis of farnesyl pyrophosphate (19). Addition of alendronate led to substantial changes in the volatome of *A. fumigatus* (Fig. 1F and G and 2D). Unexpectedly, a strong increase in the release of sesquiterpenes (represented by peaks 13 and 16 in Fig. 2) was observed up to a concentration of 313 μg/ml. At higher concentrations, sesquiterpene release was significantly reduced, whereas the concentrations of monoterpenes reached 30- to 40-fold the amounts of the drug-free control. At the same time, VOCs that were completely absent in the absence of this drug arose: a new and highly abundant monoterpene was identified as β-pinene (peak 70), and it appeared at concentrations that began to affect growth. From an alendronate concentration of 313 μg/ml and higher, C_5 compounds (peaks 67 to 69) accumulated in the samples. Moreover, weak but well-identifiable signals from acyclic monoterpene derivatives unique to this culture condition were identified (peaks 74 to 78). This increased production of hemi- and monoterpenes reflects well the metabolic distortions that appear in the presence of alendronate at concentrations high enough to inhibit sesquiterpene production.

As expected, voriconazole, an inhibitor of ergosterol biosynthesis (which is a metabolic event occurring downstream of the farnesyl pyrophosphate metabolism), did not affect the production of the volatiles (Fig. 2B).

(ii) Mutant strains. A molecular approach was undertaken to complement the assays of inhibition of terpene production by drugs and to identify genes that are responsible for VOC production.

(a)* ΔAFUA_8G00520 *terpene cyclase mutant. The terpene cyclase encoded by *AFUA_8G00520* was previously identified to be a key enzyme in the biosynthesis of the secondary metabolite fumagillin (13). Using a *Saccharomyces cerevisiae* strain producing the recombinant protein and farnesyl pyrophosphate as a substrate, these authors showed that the sesquiterpene β-*trans*-bergamotene is the product of the enzyme. Furthermore, when assayed by SPME-GC/MS, the volatome of the *A. fumigatus* terpene

FIG 2 Influence of cations and drugs on the production of major VOCs. (A) Release of the monoterpenes α-pinene (peak 4), camphene (peak 5), and the sesquiterpenes α-bergamotene (peak 13) and β-*trans*-bergamotene (peak 16) in the presence of increased divalent cation concentrations. (Left) VOC amounts; (right) fungal biomasses. The values in parentheses on the *x* axis indicate the fold change in VOC production levels relative to the amount produced on regular Brian's broth (Bri). (B to D) VOC production in the presence of different concentrations of voriconazole, pravastatin, and alendronate. The lower graph in panel D shows the production of untypical VOCs at a high alendronate concentration. Due to their absence under control conditions, quantitative data for isoprenol (peak 67), prenol (peak 68), and β-pinene (peak 70) are given as percentages of the maximal concentration detected.

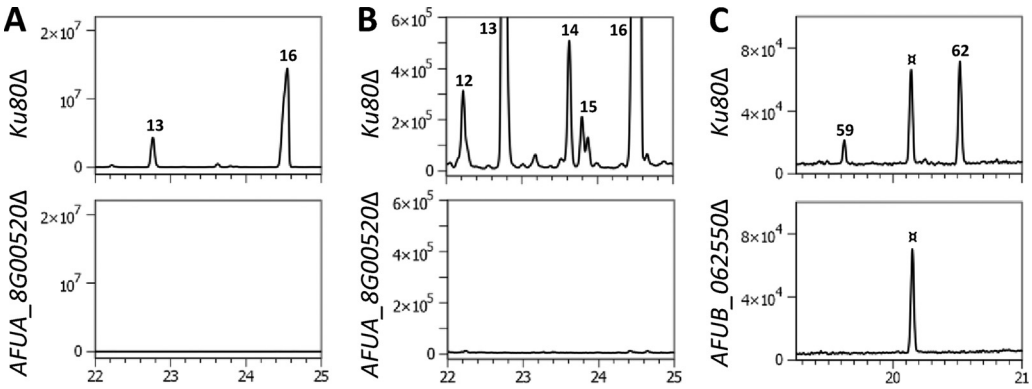

FIG 3 SPME-GC/MS analysis of terpene biosynthesis mutants of *Aspergillus fumigatus*. *x* axis, time (in minutes); *y* axis, ion count. Contaminants are indicated by ¤. (A, B) Profile of the mutant strain deficient in terpene cyclase AFUA_8G00520 (the *AFUA_8G00520*Δ mutant). Panels A and B show the same chromatogram sections at different signal intensity scales. The strain did not produce either the major compounds at peaks 13 and 16 (A) or the less abundant sesquiterpenes (B). (C) Profile of the mutant strain deficient in terpene synthase AFUB_062550 (the *AFUB_062550*Δ mutant). The strain did not produce compounds identified as diterpenes (peaks 59 and 62).

cyclase-deficient mutant lacked all peaks that were assigned to sesquiterpenes (Fig. 3A and B). Not only the β-*trans*-bergamotene but also all the other sesquiterpenoid compounds were absent, showing that the production of all sesquiterpenes was under the control of a unique terpene cyclase. The production of monoterpenes was not affected by this gene deletion.

***(b)* ΔAFUB_062550 *terpene synthase mutant*.** BLAST analysis showed that terpene synthases are not very conserved and share little similarity between species. In the genome of *A. fumigatus*, we identified a putative terpene synthase encoded by *AFUB_062550* that showed little sequence similarity to the prenyltransferases of *Zea mays* (e.g., GenBank accession number DAA49971.1) but was similar to copalyl-diphosphate/kaurene synthetases from the *Gibberella fujikuroi* species complex (e.g., *Fusarium proliferatum* kaurene synthetase, GenBank accession number CAP74389.1). The protein encoded by *AFUB_062550* contained a partial *ent*-copalyldiphosphate synthase domain (CDD PLN02592), indicating that it is involved in diterpene synthesis. We undertook the deletion of this gene and assayed the mutant for changes in the volatome. The gene deletion mutant showed no growth differences, lacked an apparent phenotype, and still produced mono- and sesquiterpenes. In contrast, the mutant lacked the diterpene signals that occur when the fungus is grown in iron-supplemented medium (Fig. 3C). This result showed that the protein encoded by the gene *AFUB_062550* is responsible for diterpene biosynthesis.

DISCUSSION

The putative biosynthetic pathway leading to the production of the terpenes and the targets of the different drugs tested is shown in Fig. 4. The recent molecular analysis of the fumagillin biosynthesis cluster revealed that the terpene cyclase AFUA_8G00520 is responsible for the biosynthesis of the sesquiterpenoid moiety in the fumagillin molecule (13). Not only the β-*trans*-bergamotene but also all sesquiterpene signals disappeared in the Δ*AFUA_8G00520* mutant. Thus, production of sesquiterpenes is under the control of a single enzyme and inseparably linked to the production of fumagillin. In *Zea mays*, the terpene synthase TPS10 produces (*E*)-α-bergamotene and (*E*)-β-farnesene at constant ratios (20). Mutations in the catalytic center of the maize enzyme lead to changes in the ratio between the main products and the pattern of auxiliary reaction products, thus demonstrating that a single enzyme has the ability to produce multiple terpenes at characteristic ratios. In *A. fumigatus*, constant intensity ratios between sesquiterpene peaks were also observed, and deletion of a single gene led to the disappearance of all sesquiterpenes. Based on these data and the similar observation made for the maize terpene synthase, we conclude that AFUA_8G00520 alone is responsible for the production of all sesquiterpenes in *A. fumigatus*.

It is known that the production of fumagillin is under the control of VeA (21). However, we did not find a reduction of the β-*trans*-bergamotene concentration in the Δ*veA* strain under the assay conditions used in the present work. In contrast, we observed an increase of β-*trans*-bergamotene release in this mutant (data not shown). Both studies used different culture conditions, which could have caused a change in the regulatory output of VeA affecting β-*trans*-bergamotene biosynthesis.

The biosynthesis and the biological function of diterpenes and their possible derivatives have not been studied in *A. fumigatus*, but other ascomycetes are known producers of diterpene-derived secondary metabolites. *Gibberella fujikuroi* (*Fusarium moniliforme*) is a producer of gibberellic acid, which acts as a phytohormone that causes increased growth elongation in plants (22). We found in our experiments a compound identified as *ent*-kaurene (Fig. 4; see also Table S1 in the supplemental material). *ent*-Kaurene is an intermediate in gibberellic acid biosynthesis (23, 24), suggesting that metabolites related to gibberellins may also be produced by *A. fumigatus*. The deletion of *AFUB_062550* led to the disappearance of all peaks that were assigned to diterpenes, indicating a synthesis of these compounds under the control of a single enzyme, as was observed for the sesquiterpenes.

Using a sequence similarity search and conserved protein domains, we also searched for monoterpene synthases/cyclases in *A. fumigatus*. These enzymes are functionally exclusively described in plants. No genes with significant homologies to plant genes were identified in *A. fumigatus*.

In the presence of alendronate and pravastatin, the inhibition of the terpene biosynthesis pathway was not translated into a full inhibition of terpene production, even though the drug had an

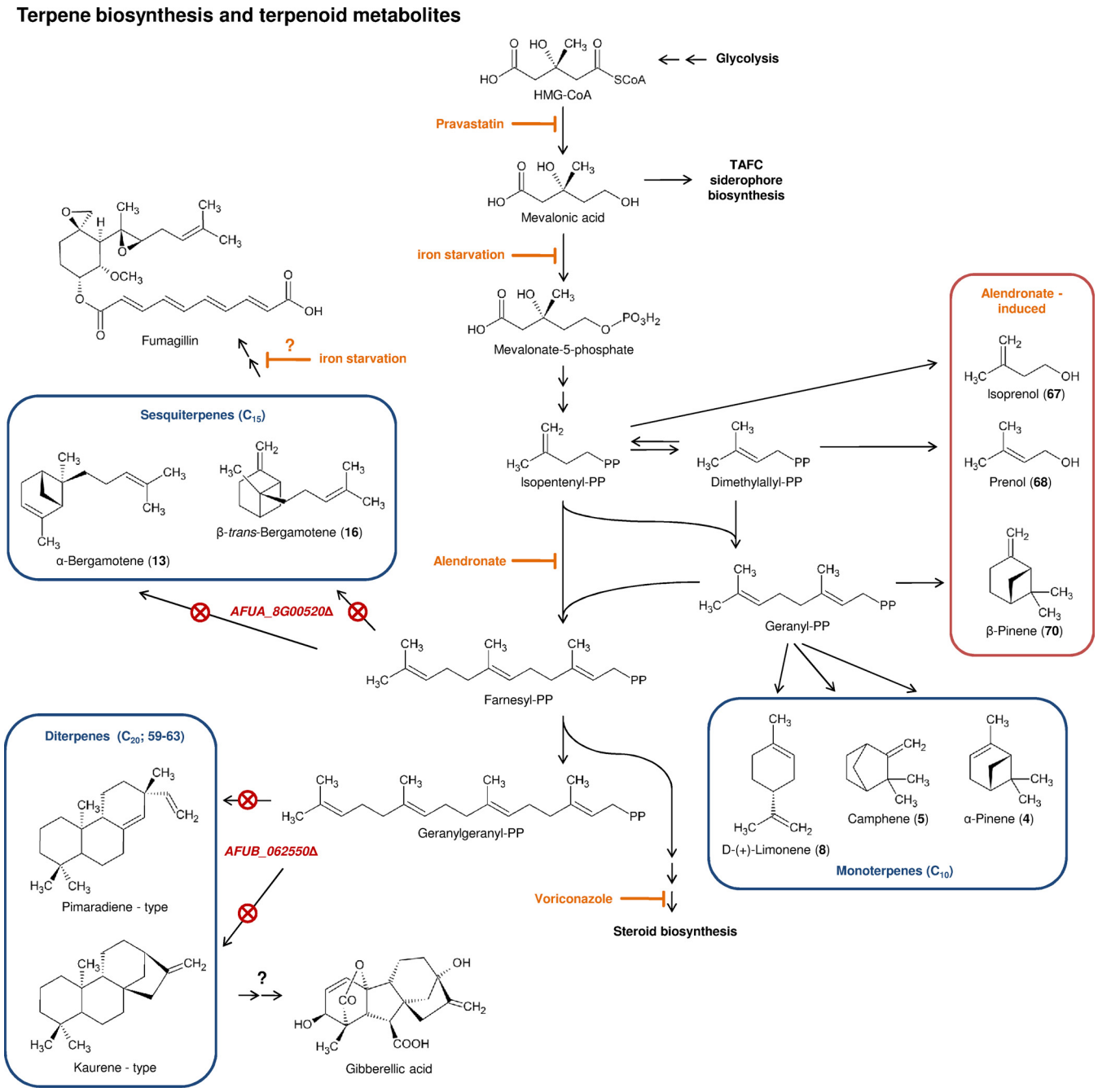

FIG 4 Metabolic pathways of VOC production in *Aspergillus fumigatus*: terpene biosynthesis and terpenoid metabolites. The production of terpenes originates in the synthesis of mevalonic acid. In this study, several drugs were used to interfere with terpenoid biosynthesis (pravastatin, alendronate, voriconazole). In two terpene synthase mutant strains, the production of specific groups of terpenes is suppressed (*AFUA_8G00520*Δ mutant, sesquiterpenes; *AFUB_062550*Δ mutant, diterpenes). Bold numbers in parentheses correspond to the entries in Table 1 and the GC peaks shown in Fig. 1. CoA, coenzyme A; PP, pyrophosphate.

effect on vegetative growth. When the fungus was grown in Brian's medium in the presence of 31 μg/ml and 63 μg/ml pravastatin and 313 μg/ml alendronate, where we saw the release of the largest amounts of volatiles, growth was reduced but not fully inhibited. Moreover, at these concentrations, quantitative PCR experiments showed that the gene responsible for the production of the sesquiterpenes, *AFUA_8G00520*, was expressed at levels close to those for the control (data not shown). This result demonstrates that the enzyme responsible for the production of these VOCs is still present and active. The relative increase in VOC release may also be linked to the production of a larger amount of the terpene cyclase substrate under stress conditions induced by the drug. In this case, even though the upstream pathway is partially inhibited, the induction of sesquiterpene production outweighs the inhibitory effect. At the highest drug concentrations, this paradoxical effect disappeared (Fig. 2).

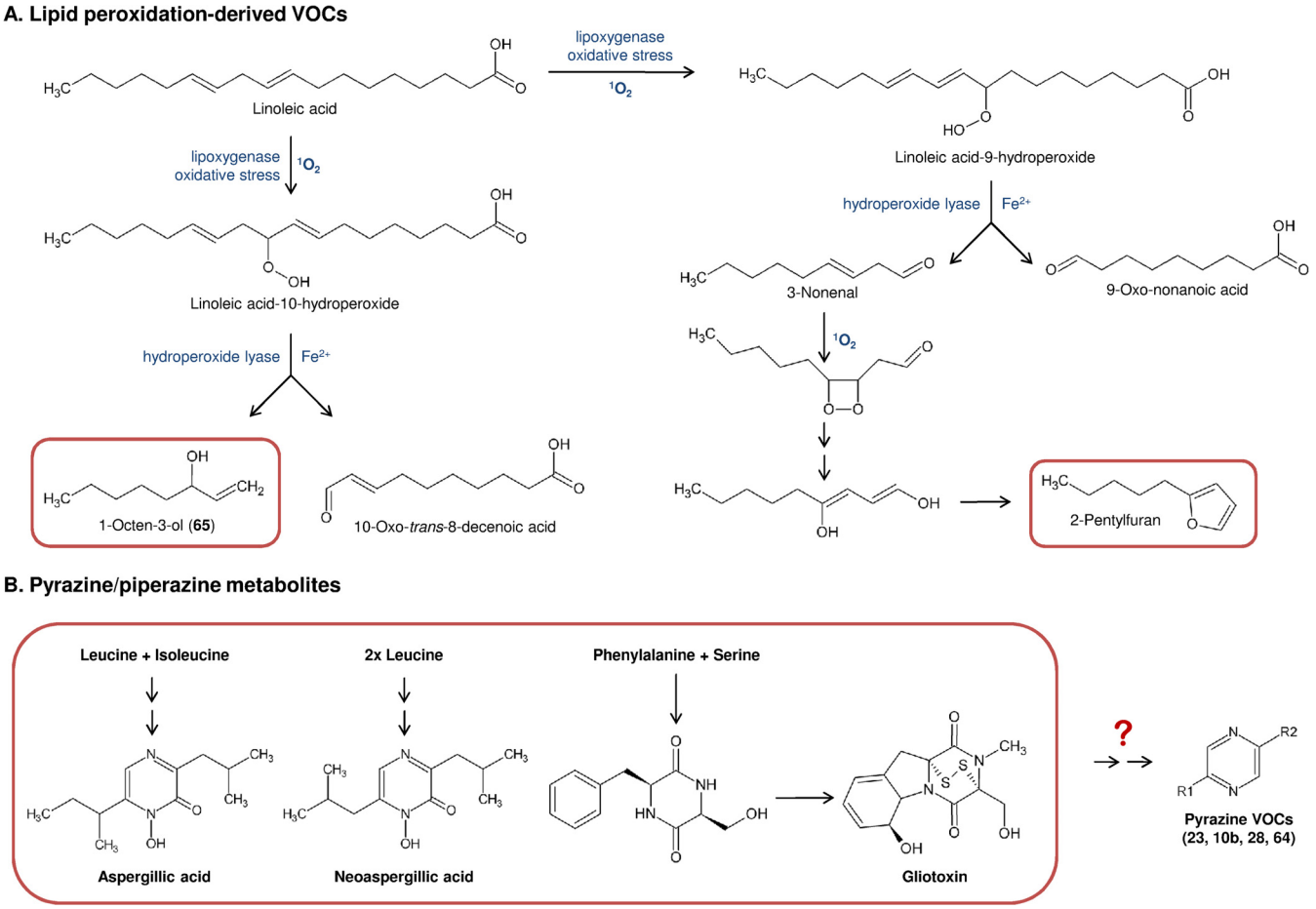

FIG 5 Metabolic pathways leading to VOC production in *Aspergillus fumigatus*: lipid peroxidation products and pyrazines. Bold numbers in parentheses correspond to the entries in Table 1 and the GC peaks shown in Fig. 1. (A) Enzymatic or nonenzymatic oxidative breakdown of unsaturated fatty acids (here, linoleic acid) leads to volatile degradation products. A fungus-specific pathway leads to 1-octen-3-ol, whereas 2-pentylfuran is produced by plants and nonenzymatic oxidative lipid breakdown. (B) *A. fumigatus* produces several compounds containing pyrazine/piperazine heterocycles that may be the origin for the VOCs identified as pyrazines.

It is was previously reported that divalent cations have an influence on the production of mycotoxins/secondary metabolites in several ascomycetes, including members of the *Aspergillus* genus (25). When adding iron, we observed the same with respect to sesquiterpenes. Uptake of iron is tightly connected to siderophore production, and the biosynthesis of the siderophore triacetylfusarinine C (TAFC) is linked to the mevalonate pathway. It was shown that the siderophore production induced by the lack of available iron cross-activated the mevalonate pathway and hereby increased the amount of 3-hydroxy-3-methylglutaryl coenzyme A (HMG-CoA) reductase (26). In contrast, iron starvation decreased the transcript levels of the mevalonate kinase gene (*AFUA_4G07780*) and thereby inhibited terpene biosynthesis. A derepression under iron supplementation would lead to overall increased terpene production, which is in accordance with our observations (Fig. 1A to C and 3A). Both effects of an elevated iron concentration—the moderate increase in monoterpene release and the strong induction of sesquiterpene production—were also present in mutants of siderophore biosynthesis (*sidA*Δ, *sidC*Δ, *sidD*Δ, and *sidF*Δ mutants), indicating that this effect is not associated with siderophore production (data not shown).

In our experiments, some VOCs that did not originate from terpene biosynthesis were associated with elevated iron concentrations and a facilitated access to oxygen. We observed the formation of 1-octene-3-ol and its isomer, 3-octanone, when *A. fumigatus* was grown in a 1-liter fermentor containing minimal medium. In vial cultivations, those compounds were only occasionally detected in plugged (permeable) vials after 2 days of cultivation but were more abundant after 3 and 4 days (data not shown). Thus, we believe that their occurrence relies on extended cultivation and/or the presence of oxygen. Our hypothesis is that these compounds originate from lipid peroxidation that relies on the presence of oxygen (Fig. 5). In mushrooms, 1-octen-3-ol is a product of enzyme-driven oxidative breakdown of linoleic acid (Fig. 5A) (27).

Although 2-pentylfuran (2-PF) was reported to be produced when *A. fumigatus* was grown *in vitro* on blood agar (9) and to be present in the breath of aspergillosis patients, 2-PF was never detected in our studies. However, the possibility that it could originate from a nonspecific inflammatory process is questioned, especially since this compound can be a product of nonenzymatic oxidation of linoleic acid (Fig. 5A, pathway on the right) (28–30).

We observed the release of 2-PF from medium containing bovine serum albumin (data not shown). This result suggests that 2-PF can originate from blood hemoglobin, especially hemorrhages of inflamed tissues, rather than being produced by the fungus itself.

Several compounds that occurred in iron-enriched aerated cultures have been identified as pyrazines. Their production is not related to terpene biosynthesis or lipid breakdown but potentially originates from the formation of cyclodipeptides. This cyclization is catalyzed by nonribosomal peptide synthetases and initially leads to the formation of a diketopiperazine. In *A. fumigatus*, gliotoxin is produced from serine and phenylalanine and contains such a diketopiperazine core structure that is further modified to contain a functionally essential disulfide bridge (31). A diketopiperazine heterocycle can be partially reduced, as it occurs in aspergillic acid. Those compounds are products of the cyclodimerization of leucine and isoleucine and were isolated from *Aspergillus flavus* (32, 33). Similarly, pulcherriminic acid, a dihydroxypyrazine produced by *Candida pulcherrima*, is formed by cyclization of two leucines (34) (Fig. 5B). Metabolic pathways leading from piperazines to aromatic pyrazines are not described in *A. fumigatus*, and so it remains to be elucidated if the detected VOCs are metabolically related to the above-mentioned secondary metabolites.

ACKNOWLEDGMENTS

We thank Yi Tang (University of California, Los Angeles) for sending the β-*trans*-bergamotene standard.

This work was supported by the ERA-NET PathoGenoMics aspBIOmics project.

REFERENCES

1. **White PL, Parr C, Thornton C, Barnes RA.** 2013. Evaluation of real-time PCR, galactomannan enzyme-linked immunosorbent assay (ELISA), and a novel lateral-flow device for diagnosis of invasive aspergillosis. J. Clin. Microbiol. **51:**1510–1516. http://dx.doi.org/10.1128/JCM.03189-12.
2. **Goeminne PC, Vandendriessche T, Van Eldere J, Nicolai BM, Hertog ML, Dupont LJ.** 2012. Detection of *Pseudomonas aeruginosa* in sputum headspace through volatile organic compound analysis. Respir. Res. **13:** 87. http://dx.doi.org/10.1186/1465-9921-13-87.
3. **Zhu J, Bean HD, Wargo MJ, Leclair LW, Hill JE.** 2013. Detecting bacterial lung infections: *in vivo* evaluation of *in vitro* volatile fingerprints. J. Breath Res. **7:**016003. http://dx.doi.org/10.1088/1752-7155/7/1/016003.
4. **Hakim M, Broza YY, Barash O, Peled N, Phillips M, Amann A, Haick H.** 2012. Volatile organic compounds of lung cancer and possible biochemical pathways. Chem. Rev. **112:**5949–5966. http://dx.doi.org/10.1021/cr300174a.
5. **Liu H, Wang H, Li C, Wang L, Pan Z, Wang L.** 2014. Investigation of volatile organic metabolites in lung cancer pleural effusions by solid-phase microextraction and gas chromatography/mass spectrometry. J. Chromatogr. B Analyt. Technol. Biomed. Life Sci. **945–946:**53–59. http://dx.doi.org/10.1016/j.jchromb.2013.11.038.
6. **Gao P, Korley F, Martin J, Chen BT.** 2002. Determination of unique microbial volatile organic compounds produced by five *Aspergillus* species commonly found in problem buildings. AIHA J. (Fairfax, Va.) **63:**135–140. http://dx.doi.org/10.1080/15428110208984696.
7. **Polizzi V, Adams A, De Saeger S, Van Peteghem C, Moretti A, De Kimpe N.** 2012. Influence of various growth parameters on fungal growth and volatile metabolite production by indoor molds. Sci. Total Environ. **414:**277–286. http://dx.doi.org/10.1016/j.scitotenv.2011.10.035.
8. **Polizzi V, Adams A, Malysheva SV, De Saeger S, Van Peteghem C, Moretti A, Picco AM, De Kimpe N.** 2012. Identification of volatile markers for indoor fungal growth and chemotaxonomic classification of *Aspergillus* species. Fungal Biol. **116:**941–953. http://dx.doi.org/10.1016/j.funbio.2012.06.001.
9. **Chambers ST, Syhre M, Murdoch DR, McCartin F, Epton MJ.** 2009. Detection of 2-pentylfuran in the breath of patients with *Aspergillus fumigatus*. Med. Mycol. **47:**468–476. http://dx.doi.org/10.1080/13693780802475212.
10. **Bazemore RA, Feng J, Cseke L, Podila GK.** 2012. Biomedically important pathogenic fungi detection with volatile biomarkers. J. Breath Res. **6:**016002. http://dx.doi.org/10.1088/1752-7155/6/1/016002.
11. **Koo S, Thomas HR, Rearden P, Comolli J, Baden LR, Marty FM.** 2012. Breath volatile organic compound (VOC) profiles for the diagnosis of invasive aspergillosis (IA), abstr. M-1060. Abstr. 52nd Intersci. Conf. Antimicrob. Agents Chemother., San Francisco, CA. American Society for Microbiology, Washington, DC.
12. **da Silva Ferreira ME, Kress MR, Savoldi M, Goldman MH, Härtl A, Heinekamp T, Brakhage AA, Goldman GH.** 2006. The *akuB*(KU80) mutant deficient for nonhomologous end joining is a powerful tool for analyzing pathogenicity in *Aspergillus fumigatus*. Eukaryot. Cell **5:**207–211. http://dx.doi.org/10.1128/EC.5.1.207-211.2006.
13. **Lin HC, Chooi YH, Dhingra S, Xu W, Calvo AM, Tang Y.** 2013. The fumagillin biosynthetic gene cluster in *Aspergillus fumigatus* encodes a cryptic terpene cyclase involved in the formation of β-*trans*-bergamotene. J. Am. Chem. Soc. **135:**4616–4619. http://dx.doi.org/10.1021/ja312503y.
14. **Hartmann T, Dümig M, Jaber BM, Szewczyk E, Olbermann P, Morschhäuser J, Krappmann S.** 2010. Validation of a self-excising marker in the human pathogen *Aspergillus fumigatus* by employing the beta-rec/six site-specific recombination system. Appl. Environ. Microbiol. **76:**6313–6317. http://dx.doi.org/10.1128/AEM.00882-10.
15. **Lambou K, Perkhofer S, Fontaine T, Latge JP.** 2010. Comparative functional analysis of the OCH1 mannosyltransferase families in *Aspergillus fumigatus* and *Saccharomyces cerevisiae*. Yeast **27:**625–636. http://dx.doi.org/10.1002/yea.1798.
16. **Brian PW, Dawkins AW, Grove JF, Hemming HG, Lowe D, Norris GLF.** 1961. Phytotoxic compounds produced by *Fusarium equiseti*. J. Exp. Bot. **12:**1–12. http://dx.doi.org/10.1093/jxb/12.1.1.
17. **Cove DJ.** 1966. The induction and repression of nitrate reductase in the fungus *Aspergillus nidulans*. Biochim. Biophys. Acta **113:**51–56. http://dx.doi.org/10.1016/S0926-6593(66)80120-0.
18. **Clavaud C, Beauvais A, Barbin L, Munier-Lehmann H, Latgé JP.** 2012. The composition of the culture medium influences the β-1,3-glucan metabolism of *Aspergillus fumigatus* and the antifungal activity of inhibitors of β-1,3-glucan synthesis. Antimicrob. Agents Chemother. **56:**3428–3431. http://dx.doi.org/10.1128/AAC.05661-11.
19. **van Beek ER, Cohen LH, Leroy IM, Ebetino FH, Löwik CW, Papapoulos SE.** 2003. Differentiating the mechanisms of antiresorptive action of nitrogen containing bisphosphonates. Bone **33:**805–811. http://dx.doi.org/10.1016/j.bone.2003.07.007.
20. **Köllner TG, Gershenzon J, Degenhardt J.** 2009. Molecular and biochemical evolution of maize terpene synthase 10, an enzyme of indirect defense. Phytochemistry **70:**1139–1145. http://dx.doi.org/10.1016/j.phytochem.2009.06.011.
21. **Dhingra S, Lind AL, Lin HC, Tang Y, Rokas A, Calvo AM.** 2013. The fumagillin gene cluster, an example of hundreds of genes under *veA* control in *Aspergillus fumigatus*. PLoS One **8:**e77147. http://dx.doi.org/10.1371/journal.pone.0077147.
22. **Yabuta T, Sumiki Y.** 1938. On the crystal of gibberellin, a substance to promote plant growth. J. Agric. Chem. Soc. Jpn. **14:**1526.
23. **Kawaide H, Imai R, Sassa T, Kamiya Y.** 1997. *Ent*-kaurene synthase from the fungus *Phaeosphaeria* sp. L487. cDNA isolation, characterization, and bacterial expression of a bifunctional diterpene cyclase in fungal gibberellin biosynthesis. J. Biol. Chem. **272:**21706–21712.
24. **Tudzynski B, Kawaide H, Kamiya Y.** 1998. Gibberellin biosynthesis in *Gibberella fujikuroi*: cloning and characterization of the copalyl diphosphate synthase gene. Curr. Genet. **34:**234–240. http://dx.doi.org/10.1007/s002940050392.
25. **Cuero R, Ouellet T.** 2005. Metal ions modulate gene expression and accumulation of the mycotoxins aflatoxin and zearalenone. J. Appl. Microbiol. **98:**598–605. http://dx.doi.org/10.1111/j.1365-2672.2004.02492.x.
26. **Yasmin S, Alcazar-Fuoli L, Gründlinger M, Puempel T, Cairns T, Blatzer M, Lopez JF, Grimalt JO, Bignell E, Haas H.** 2012. Mevalonate governs interdependency of ergosterol and siderophore biosyntheses in the fungal pathogen *Aspergillus fumigatus*. Proc. Natl. Acad. Sci. U. S. A. **109:**E497–E504. http://dx.doi.org/10.1073/pnas.1106399108.
27. **Wurzenberger M, Grosch W.** 1984. The formation of 1-octen-3-ol from the 10-hydroperoxide isomer of linoleic acid by a hydroperoxidelyase in

mushrooms (*Psalliotabispora*). Biochim. Biophys. Acta **794:**25–30. http://dx.doi.org/10.1016/0005-2760(84)90293-5.
28. **Min DB, Callison AL, Lee HO.** 2003. Singlet oxygen oxidation for 2-pentylfuran and 2-pentenyfuran formation in soybean oil. J. Food Sci. **68:** 1175–1178. http://dx.doi.org/10.1111/j.1365-2621.2003.tb09620.x.
29. **Chambers ST, Bhandari S, Scott-Thomas A, Syhre M.** 2011. Novel diagnostics: progress toward a breath test for invasive *Aspergillus fumigatus*. Med. Mycol. **49**(Suppl 1)**:**S54–S61. http://dx.doi.org/10.3109/13693786.2010.508187.
30. **Bhandari S, Chambers S, Pearson J, Syhre M, Epton M, Scott-Thomas A.** 2011. Determining the limits and confounders for the 2-pentylfuran breath test by gas chromatography/mass spectrometry. J. Chromatogr. B Analyt. Technol. Biomed. Life Sci. **879:**2815–2820. http://dx.doi.org/10.1016/j.jchromb.2011.08.010.
31. **Scharf DH, Heinekamp T, Remme N, Hortschansky P, Brakhage AA, Hertweck C.** 2012. Biosynthesis and function of gliotoxin in *Aspergillus fumigatus*. Appl. Microbiol. Biotechnol. **93:**467–472. http://dx.doi.org/10.1007/s00253-011-3689-1.
32. **Dutcher JD.** 1958. Aspergillic acid; an antibiotic substance produced by *Aspergillus flavus*. J. Biol. Chem. **232:**785–795.
33. **MacDonald JC.** 1961. Biosynthesis of aspergillic acid. J. Biol. Chem. **236:** 512–514.
34. **MacDonald JC.** 1965. Biosynthesis of pulcherriminic acid. Biochem. J. **96:**533–538.